

MIT Open Access Articles

Stochastic and deterministic causes of streamer branching in liquid dielectrics

The MIT Faculty has made this article openly available. **Please share** how this access benefits you. Your story matters.

Citation: Jadidian, Jouya, Markus Zahn, Nils Lavesson, Ola Widlund, and Karl Borg. "Stochastic and deterministic causes of streamer branching in liquid dielectrics." *Journal of Applied Physics* 114, no. 6 (2013): 063301. © 2013 AIP Publishing LLC

As Published: <http://dx.doi.org/10.1063/1.4816091>

Publisher: American Institute of Physics (AIP)

Persistent URL: <http://hdl.handle.net/1721.1/80813>

Version: Final published version: final published article, as it appeared in a journal, conference proceedings, or other formally published context

Terms of Use: Article is made available in accordance with the publisher's policy and may be subject to US copyright law. Please refer to the publisher's site for terms of use.



Stochastic and deterministic causes of streamer branching in liquid dielectrics

Jouya Jadian,^{1,a)} Markus Zahn,¹ Nils Lavesson,² Ola Widlund,² and Karl Borg²

¹*Department of Electrical Engineering and Computer Science, MIT, Cambridge, Massachusetts 02139, USA*

²*ABB Corporate Research, Västerås SE 72178, Sweden*

(Received 9 May 2013; accepted 21 June 2013; published online 8 August 2013)

Streamer branching in liquid dielectrics is driven by stochastic and deterministic factors. The presence of stochastic causes of streamer branching such as inhomogeneities inherited from noisy initial states, impurities, or charge carrier density fluctuations is inevitable in any dielectric. A fully three-dimensional streamer model presented in this paper indicates that deterministic origins of branching are intrinsic attributes of streamers, which in some cases make the branching inevitable depending on shape and velocity of the volume charge at the streamer frontier. Specifically, any given inhomogeneous perturbation can result in streamer branching if the volume charge layer at the original streamer head is relatively thin and slow enough. Furthermore, discrete nature of electrons at the leading edge of an ionization front always guarantees the existence of a non-zero inhomogeneous perturbation ahead of the streamer head propagating even in perfectly homogeneous dielectric. Based on the modeling results for streamers propagating in a liquid dielectric, a gauge on the streamer head geometry is introduced that determines whether the branching occurs under particular inhomogeneous circumstances. Estimated number, diameter, and velocity of the born branches agree qualitatively with experimental images of the streamer branching. © 2013 AIP Publishing LLC. [<http://dx.doi.org/10.1063/1.4816091>]

I. INTRODUCTION

Streamers are thin fast elongating structures with semi-spherical heads that form in regions of dielectric that are ionized by intense electric fields.^{1,2} Streamer heads propagate as ionization waves with velocities much higher than the maximum drift velocity of electrons.³ Their spatial structure is inherently three-dimensional as they easily branch out and become asymmetric. Streamer branching can occur due to both deterministic and stochastic origins in low and high density gases, liquids and even solids.^{4–12} The complex nature and structure of liquids has inhibited the development of a comprehensive streamer theory in liquid state. Rather, scientists have derived understanding of the basic processes (e.g., ionization) and the complex phenomena (e.g., streamer branching) in liquids by utilizing theories from both the solid-state or compressed gas-state. Streamer research in the gas-state, in particular, is usually one step ahead of the liquid-state.^{6–8} For instance, the ionization mechanisms are well known in gas state (both low and high pressure gases), while in liquids we have to incorporate a solid-state ionization theorem.³ Specifically, over the last two decades, researchers have enlightened the mechanisms behind the streamer propagation and branching in gases.^{6,7,10,11} Moreover, significant improvements in advanced stereo-photography of streamers¹² have been used as an enabling tool to investigate the main origins of streamer branching in gases. Experimental photography of streamers in liquid dielectrics, on the other hand, has proven more difficult over the years.^{1–4} Numerical modeling seems to be an appropriate alternative for rendering understandable three-dimensional images that reveal the main causes of streamer branching as they have been

successfully used for gaseous media before.¹⁰ Modeling of streamer branching is attractive amongst many different disciplines due to its complexity and importance in discharge physics.^{5–17} Some of the examples of the most effective modeling and analytical approaches are fractal morphology of streamer trees,¹⁴ conformal mapping,⁹ electro-hydrodynamic modeling with or without cylindrical symmetry,^{5,13} moving boundary approximation,⁸ particle models,¹⁰ macroscopic inhomogeneities,¹³ realistic fluctuations,⁶ slow branching in deterministic fluid models,¹⁵ multiphase fingering driven by small signal interfacial waves;^{16,17} each revealing important aspects of the streamer branching. However, none of these studies is capable of giving a thorough answer to the question of how and to what extent deterministic and stochastic elements contribute to the streamer branching. This paper presents a fully three-dimensional (3-D) model that enables us to investigate stochastic and deterministic causes of the streamer branching. Figure 1 compares a properly taken experimental image of a streamer tree formed in a liquid dielectric,¹⁶ with a corresponding result of our model, obtained under reasonably similar conditions of dielectric medium, gap distance, electrode geometry and the applied voltage. The streamer branch diameters from optical measurements is estimated to be about half of the electrodynamic diameters, as the model describes. The streamer column diameters, number of branches and the angle between branches meaningfully resemble the experimental image.

Initiation of streamer branching requires a finite perturbation.^{5,6,13} If there is absolutely no perturbation around the streamer head, which is practically unlikely, in some cases, the propagation of the streamer in a single column becomes impossible, i.e., the streamer head becomes bushy and the propagation velocity drops significantly due to the shielding effect of the volume charge.³ Two-dimensional models of

^{a)}Email: jouya@mit.edu

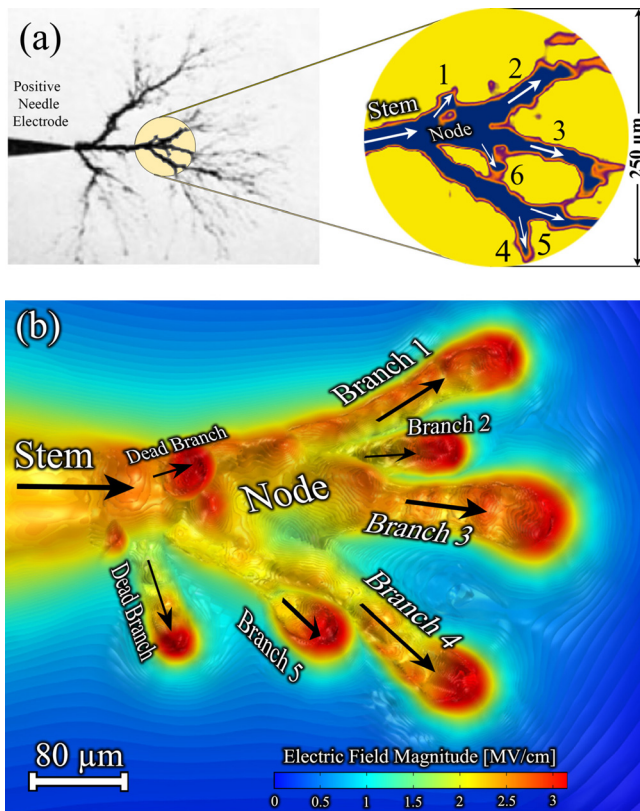


FIG. 1. Typical view of positive streamer branching in a liquid dielectric. (a) Experimental image of a positive streamer initiated from a needle electrode^{16,18,36} and (b) 3-D modeling result of a corresponding case (iso-surface plot of the electric field distribution). The streamer structures are qualitatively similar in experiments and simulations. The fractal structure of the streamer tree in the experimental image makes it possible to compare the modeling result also with other nodes of the tree including the one at the needle electrode tip.

streamer with cylindrical symmetry normally suffer from lack of asymmetric perturbations especially at high levels of applied voltage peak.^{19,20} Required perturbations can be inherited from the inhomogeneous initial states (such as an initial electron density fluctuation^{4,6}), macroscopic impurity perturbations (such as dust particles, air bubbles, water droplets, or other macroscopic objects^{5,13}), or variations of dielectric densities or molecule alignment.^{3,4} Our 3-D modeling results show that microscopic inhomogeneities (smaller than $10\ \mu\text{m}$) initiate streamer branches in liquid dielectrics whose characteristics clearly resemble their parents. Macroscopic inhomogeneities (larger than $10\ \mu\text{m}$), on the other hand, dominantly determine the branches' structure and velocity. Macroscopic perturbations, which are rare in practice,^{3,4} appreciably decrease the sensitivity of branching dynamics to the applied voltage and even geometry of the electrodes. Most of the experimental references of this paper do not include large inhomogeneities, since the results obtained from the microscopic inhomogeneities reasonably match better with respective experimental records.

Current theoretical understanding of streamer branching is presented in Sec. II as well as the 3-D model used for study of the positive streamer branching. The focus of this paper is on the streamer branching in transformer oil; however, the model and its results can be generalized to other

dielectric media. The effects of the applied voltage peak (up to five times larger than 50 percent breakdown voltage, U_{BD} (Ref. 3)), rise-time (from 1 ns to $0.1\ \mu\text{s}$), the electrode geometry and gap distance are investigated on the shape of the streamer tree, the number, diameter, and velocity of the branches in a needle-sphere electrode geometry as given in Sec. III. Post processing of the results indicates that there is a clear correlation between the characteristics of the main streamer stem (also known as leader in the literature) just before branching and the attributes of the born branches. This correlation is discussed in detail in Sec. IV as deterministic causes of branching.

In numerical modeling, the actual branching triggered by the physical perturbations must be distinguished from the artifacts developed by numerical instabilities. As addressed in Sec. IV, several sanity checks are performed to ensure that the physical elements are the only initiators of the observed branching in the model. The modeling results have been verified with experimental measurements wherever the actual data is available. The paper concludes in Sec. V with a summary of the key results.

II. THEORETICAL BACKGROUND

Theoretically, streamers can branch in fully deterministic models through Laplacian instability that resembles the underlying mechanism of viscous finger branching of a two-fluid Hele-Shaw flow⁶ or in an electro-hydrodynamic version of Rayleigh-Taylor instability with superposed charge layers.^{16,17} Such instabilities can develop when the volume charge layer ahead of the streamer front is much thinner than the streamer head radius of curvature. In the extreme case of a planar ionization front, an infinitesimal perturbation is enough to initiate a branching instability,⁶ but for a semi-spherical streamer head with a finite radius of curvature, only perturbations larger than a certain threshold can trigger a self-sustaining streamer branching.

In practice, even in carefully filtered ambient, microscopic perturbations are still present. Most of these microscopic inhomogeneities can be categorized into two main classes: (1) perturbations on the material spatial properties (presumably permittivity) and (2) fluctuations of the charge carrier density or the ionization potential.³ We have incorporated both of these inhomogeneous cases into the modeling. In applications that are of interest in industry, the macroscopic inhomogeneities inside dielectrics are usually avoided unless breakdown is desirable. Previous studies show that the macroscopic perturbations such as air bubbles or water droplets certainly deviate the streamer paths and most probably initiate the branching. In this paper we focus on microscopic inhomogeneities, which are more complex and also are much harder to avoid even in extremely purified media used for electric power insulation, such as transformer oil or SF_6 .

A. Description of the model

Our 3-D electro-hydrodynamic model is built upon the previously developed two-dimensional (2-D) streamer model,^{3,19–22} which successfully explained numerous aspects

of streamers, except for the branching phenomena. The governing equations are based on the drift-dominated charge continuity Eqs. (1)–(3) for positive ion (ρ_p), negative ion (ρ_n), and electron (ρ_e) charge densities, coupled through Gauss' law (4). The thermal diffusion Eq. (5) is included to model temperature variations (T) in oil due to Ohmic dissipation. The negative ion and electron charge densities in the governing equations are both negative quantities. The governing equations have been solved using a finite element approach²³

$$\frac{\partial \rho_p}{\partial t} + \nabla \cdot (\rho_p \mu_p \bar{E}) = G_M(|\bar{E}|) + \frac{\rho_p \rho_e R_{pe}}{q} + \frac{\rho_p \rho_n R_{pn}}{q}, \quad (1)$$

$$\frac{\partial \rho_n}{\partial t} - \nabla \cdot (\rho_n \mu_n \bar{E}) = \frac{\rho_e}{\tau_a} - \frac{\rho_p \rho_n R_{pn}}{q}, \quad (2)$$

$$\frac{\partial \rho_e}{\partial t} - \nabla \cdot (\rho_e \mu_e \bar{E}) = -G_M(|\bar{E}|) - \frac{\rho_p \rho_e R_{pe}}{q} - \frac{\rho_e}{\tau_a}, \quad (3)$$

$$\nabla \cdot (\varepsilon \bar{E}) = \rho_p + \rho_n + \rho_e, \quad (4)$$

$$\frac{\partial T}{\partial t} + v \cdot \nabla T = \frac{1}{\rho_l c_v} (k_T \nabla^2 T + \bar{E} \cdot \bar{J}), \quad (5)$$

where q , E , v , ε , k_T , c_v , and ρ_l are magnitude of electronic charge, local electric field, oil velocity, permittivity ($2.2 \varepsilon_0$), thermal conductivity, specific heat, and mass density, respectively. Representative values for transformer oil are listed in Table I. In the microsecond time scales of interest for streamer formation, the oil velocity is negligible such that $v = 0$. The parameters μ_p , μ_n , and μ_e are the mobilities of the positive ions, negative ions, and electrons, respectively. The ion-ion recombination constant, R_{pn} , is obtained from the Langevin-Debye relationship^{20,24}

$$R_{pn} = q(\mu_n + \mu_p)/\varepsilon. \quad (6)$$

The ion-electron recombination constant, R_{pe} , is assumed equal to the ion-ion recombination constant, since using the Langevin-Debye relationship for the ion-electron recombination rate leads to some overestimation.²⁰ In addition to recombination with positive ions, electrons also combine

with neutral molecules to form negative ions. This process is described as an electron attachment time constant, τ_a .^{15,20}

The generation and recombination rates play a key role in describing streamer dynamics. In spite of the recombination rates that are defined by constants, the field ionization charge density rate source term, G_M , is modeled using the Zener model of electron tunneling in solids that is improved by using the Density Functional Theory (DFT)^{3,9,25,26}

$$G_M(|\bar{E}|) = \frac{q^2 n_0 a |\bar{E}|}{h} \exp \left(-\frac{\pi^2 m^* a}{q h^2} \left(\frac{\Delta}{\sqrt{|\bar{E}|}} - \gamma \right)^2 \right). \quad (7)$$

All parameter definitions and values are given in Table I. Application of the generation term in the form of Eq. (7) in Eqs. (1) and (3) enables the model to describe the negative and positive streamers formed by extra high voltages.⁶

The positive electrode potential is defined by subtracting two exponential functions that create the standard lightning impulse voltage according to IEC 60060-1 (Ref. 27) as

$$V_{impulse} = K V_0 (e^{-\frac{t}{\tau_1}} - e^{-\frac{t}{\tau_2}}), \quad (8)$$

where K is a non-dimensional compensation factor to keep the peak amplitude of the impulse equal to V_0 , since in general, the maximum value of two subtracting exponential functions in Eq. (8) is not necessarily 1. The potential of the sphere electrode is set to ground potential. The top, bottom, and side insulating walls of the breakdown chamber³ have been assigned to have zero normal displacement field components ($\bar{n} \cdot \bar{D} = 0$). This boundary condition acts as a zero surface charge equation on the wall that also guarantees cylindrical symmetry. The boundary conditions for the charge transport continuity equations at electrodes are set to “convective fluxes” for all species,²³ while insulating wall boundaries are assigned to have no flux of any species. All boundaries are set to zero normal thermal diffusive flux (i.e., $\bar{n} \cdot \nabla T = 0$) making the approximation that the system is adiabatic on the time scales of interest.

Since diffusion of the charged species is assumed negligible in Eqs. (1)–(3), we have solved the conservative form

TABLE I. Physical parameters used in the streamer model.

| Symbol | Parameter | Value |
|------------------|---|---|
| n_0 | Number density of ionizable species | $1 \times 10^{23} \text{ m}^{-3}$ (Refs. 19, 20, and 24) |
| a | Molecular separation distance | $3.0 \times 10^{-10} \text{ m}$ (Refs. 19–22) |
| m^* | Effective electron mass | $0.1 \times m_e = 9.1 \times 10^{-32} \text{ kg}$ (Ref. 24) |
| Δ, γ | Ionization potential function parameters | $1.16 \times 10^{-18} \text{ J}, 1.118 \times 10^{-23} \text{ J cm}^{1/2} \text{ V}^{-1/2}$ (Refs. 3, 21, and 22) |
| R_{pn}, R_{pe} | Ion-ion and ion-electron recombination constant | $1.64 \times 10^{-17} \text{ m}^3 \text{ s}^{-1}$ (Refs. 19 and 20) |
| μ_p, μ_n | Positive and negative ion mobilities | $10^{-9} \text{ m}^2 \text{ V}^{-1} \text{ s}^{-1}$ (Refs. 19, 20, and 24) |
| μ_e | Electron mobility | $10^{-4} \text{ m}^2 \text{ V}^{-1} \text{ s}^{-1}$ (Refs. 19, 20, and 24) |
| c_v | Specific heat | $1.7 \times 10^3 \text{ J kg}^{-1} \text{ K}^{-1}$ (Ref. 24) |
| ρ_l | Oil mass density | 880 kg m^{-3} (Refs. 19 and 20) |
| k_T | Thermal conductivity | $0.13 \text{ W m}^{-1} \text{ K}^{-1}$ (Ref. 24) |
| q | Electronic charge | $1.602 \times 10^{-19} \text{ C}$ (Ref. 28) |
| h | Planck's constant | $6.626068 \times 10^{-34} \text{ m}^2 \text{ kg s}^{-1}$ (Ref. 28) |
| τ_a | Electron attachment time constant | 200 ns (Refs. 3, 15, and 20) |

of the general convection and diffusion equations with triangular quartic elements.²³ Numerical solutions of the charge continuity equations usually include spatial instabilities rather than expected smooth solutions.^{3,23} These spurious oscillations can be avoided by using artificial nonlinear crosswind diffusion (CWD) along with different types of streamline diffusion (SD) such as anisotropic, compensated streamline upwind Petrov-Galerkin (SUPG) and Galerkin least-square methods to stabilize the charge continuity equations.²³ It has been shown in Ref. 29 that CWD is more stable than other over-diffusive discontinuity-capturing techniques and leads to better numerical behavior, although it is computationally expensive due to its non-linear nature.²³ On the other hand, SD techniques effectively stabilize the system and accelerate the solution. We have applied minimal SD and CWD at the same time to optimally stabilize the numerical solution.^{3,21,22} Minimal artificial diffusion techniques are tuned to balance a tradeoff between removing nonphysical local oscillations (due to SD) and excessively smooth results just next to the walls (due to CWD). An average has been taken whenever any discrepancy is observed between results of different SD techniques mentioned above.

Two direct solvers, MUMPS and PARDISO, implemented in COMSOL Multiphysics are employed separately to solve the streamer model. These solvers are well known to be robust and memory efficient tools in parallel high performance computing.²³ These direct solvers have the advantage of more accuracy compared to iterative solvers, although they are computationally much more expensive. Since the present model contains nonsymmetrical matrices and nonlinear equations, combinations of direct and iterative solvers have been applied to speed up the solution. Three computers with a total 48 cores (~ 3.4 GHz) and 188 GB RAM are used in parallel to solve Eqs. (1)–(8).

B. Microscopic inhomogeneity implementation

The stochastic aspect of the streamer branching pertains to the spatial distribution, size, and intensity of the inhomogeneities. Therefore, the key role of stochastic inhomogeneities has to be included in the model in order to observe streamer branching. Macroscopic perturbations are less interesting than microscopic inhomogeneities from a modeling point of view for two main reasons: First, they essentially modify the extent of the streamer; second, in industrial applications macroscopic impurities are avoided. In the laboratory experiments, the cause of the branching is definitely not the macroscopic perturbations, since these experiments are undertaken in degassed chambers in which the liquid dielectric is filtered several times to eliminate any ionized traces and gas bubbles. In these experiments, the streamers grow in a continuously refreshed body of transformer oil.^{1–4,30} The stochastic nature of the streamer branching cannot be expressed in Eqs. (1)–(7), as they only cover macroscopic quantities and processes. Rather, we define and add a finite number of spherical regions (particles) whose stochastic location and intensity convert Eqs. (1)–(7) into a stochastic model. To implement stochastic perturbations in the model, we have used continuous uniform distribution functions

(rectangular probabilistic functions) and Gaussian functions to determine the location and intensity of the individual perturbations, respectively. Specifically, a set of spherical regions with certain radii (R_p in the range of $1\ \mu\text{m}$ – $10\ \mu\text{m}$) is placed in random locations inside the discharge chamber. The selected inhomogeneity density determines the number of spheres. Each of these spherical regions, which contains a volume charge perturbation, is placed at a stochastic position with coordinates located by three separate uniform distribution functions. These spherical regions have the same permittivity as the rest of the dielectric medium.

Theoretically, charge carrier density fluctuations can be originated by either discrete nature of electrons at the leading edge of an ionization front where the electron density is low⁶ or many external sources such as cosmic rays or other sources of ionizing radiation. As the background electric field increases, the field ionization generates more discrete free electrons at different locations of the dielectric that can gain enough energy to cause microscopic local ionizations. These local ionizations, occurring at background electric fields much weaker than the critical breakdown field, produce local charge densities that can be regarded as microscopic inhomogeneities. In our model, we simulate these inhomogeneities by adding a stochastic amount of charge generation rates inside spherical regions, which generates a bias charge density in them. The intensity of the perturbation charge density generation rates is determined by continuous Gaussian functions. The minimum perturbation charge generation rate (G_{Mp}) is zero and maximum generation rate of carrier charge densities is $10^{10}\ \text{Cm}^{-3}\ \text{s}^{-1}$, which is roughly one order of magnitude smaller than the generation rate at the typical positive streamer head in transformer oil.^{1–4} This stochastic perturbation rate generates inhomogeneous charge densities (ρ_{ps}) that are in agreement with results of Ref. 6 for a gaseous environment exposed to intense electric field. The result of stochastic perturbation rate in the range of zero and $10^{10}\ \text{Cm}^{-3}\ \text{s}^{-1}$ in transformer oil, considering the parameter values of Table I, generates in a maximum additional perturbation in charge density of $\sim 10^4\ \text{Cm}^{-3}$ inside the microscopic inhomogeneities.

The density of the microscopic inhomogeneities (C_p) is set to $10^{11}\ \text{m}^{-3}$. Considering the volume of the oil in the chamber, this distribution means that we have to place $\sim 10^6$ spheres which makes the number of the mesh elements too high, since the mesh inside these spheres have to be dense enough. Therefore, we chose to only place the inhomogeneities inside the pillbox close to the streamer head at which we have refined the mesh. Modeling results prove that inhomogeneities farther than 1 mm from the streamer head do not affect the streamer branching.

III. MODELING RESULTS OF STREAMER BRANCHING IN TRANSFORMER OIL

We have applied a vast variety of inhomogeneous distributions of perturbations to study the streamer branching specifically in transformer oil. The qualitative shape of the streamer tree, number and diameters of the branches and their velocities are clearly sensitive to the applied voltage

(and by a lesser extent, to the nonsymmetrical inhomogeneities). The branching time decreases as the applied voltage and/or the rate of rise of the voltage increase. For the same inhomogeneity, the applied voltage peak essentially determines the number of branches, while for the same applied voltage peak, the average angle between the propagation direction of the branches is determined by the applied voltage rate of rise. The modeling results show that deterministic causes of branching such as electrode geometry and applied voltage characteristics are as influential as stochastic elements on the propensity of streamers to branch out.

A. Needle-sphere electrode geometry

Figure 2 shows the discharge chamber geometry for which we performed the streamer modeling. The positive impulse voltage shown in Fig. 3 is applied to the needle electrode to initiate positive streamers. To verify our modeling results, we have used experimental results from needle-sphere electrode geometry with other different gap distances. As discussed in Ref. 21, with the same electrode geometry, if the ratio of the applied voltage peak over the gap distance is similar, the characteristics of streamers will be comparable.

Using ten different inhomogeneity distributions and densities obtained by ten different sets of Gaussian functions and continuous uniform distribution functions, the model has been run to study the effects of the stochastic parameters on the attributes of the just born branches.

The results of these ten different sets indicate that the deterministic roots of the streamer branching are dominant when the stochastic parameters vary within the boundaries described in Sec. II B (i.e., $|G_{Mp}| < 10^{10} \text{ Cm}^{-3} \text{ s}^{-1}$, $|\rho_{ps}| < 10^4 \text{ Cm}^{-3}$, $C_p = 10^{11} \text{ m}^{-3}$, $1 \mu\text{m} < R_p < 10 \mu\text{m}$). The qualitative shape of the streamer tree, number, and diameters of the branches and their velocities are clearly sensitive to the applied voltage (and by a lesser extent, to the inhomogeneities).

Among the simulation results, 13 cases have been selected to be compared with experimental images as shown in Fig. 4. The modeling parameters are not identical to the circumstances of the experiments, however they are reasonably similar. Specifically, the medium in which streamers

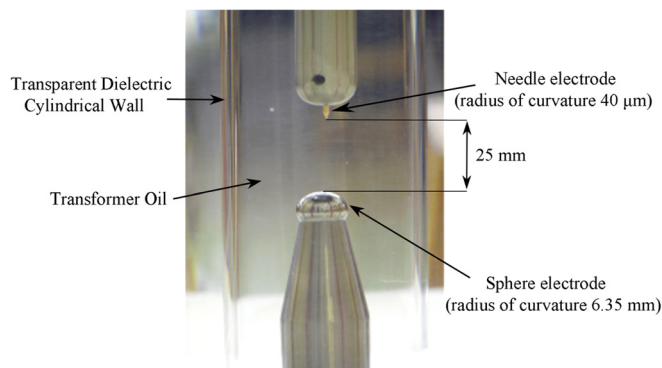


FIG. 2. Needle-sphere electrode geometry used for streamer simulation purposes as described in IEC 60897 standard.³¹ The electrodes are 25 mm apart, and the radii of curvature of the needle and sphere electrodes are 40 μm and 6.35 mm, respectively.³²

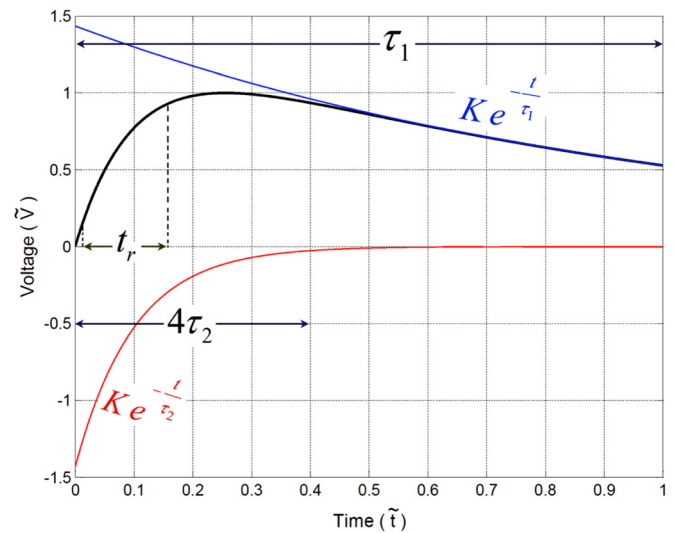


FIG. 3. IEC 60060 lightning impulse voltage (non-dimensional, $\tilde{V} = V/V_0$) with rise-time t_r (10%–90% of peak voltage) versus non-dimensional time, $\tilde{t} = t/\tau_1$ generated with subtracting two exponential functions.²⁷ In this paper, the rise-time (t_r) varies in the range of 1 ns–100 ns, while the fall-time (τ_1 is set to 1 μs for all case studies).

propagate and branch out is the same for both modeling and experimental results; the maximum electric field sensed in the gap is almost equal for pairs in each panel of Fig. 4. Currently, no approach is known to determine the distribution of inhomogeneities inside the oil. Any measurement of inhomogeneity structure would be extremely difficult since these inhomogeneities are not only functions of position, but they depend on time and electric field intensity as well. Although the inhomogeneities are not known in experimental images found in the literature, as can be seen in all the panels of Fig. 4, the structure of the streamer node and branches are qualitatively similar which suggests that density, size, and intensity of inhomogeneous perturbations in the oil have been properly chosen on realistic orders.

IV. DISCUSSION

In this section, we address two major concerns about the validity of the model. First, we answer the question of how can we ensure that the streamer branches are physical, not originated from numerical instabilities? In Sec. IV B, we devise a gauge that enables us to predict whether the branching occurs at an instantaneous time based on the geometry of the volume charge distribution at the streamer head, and if it happens, how many branches will be born.

A. Avoiding numerical instabilities: Sanity check

In numerical modeling, the actual branching caused by the physical perturbations must be distinguished from the artifacts developed by numerical instabilities. As a sanity check, we have studied the effect of several symmetric inhomogeneous charge densities in oil on the streamer branching. If the mesh is refined enough to avoid misinterpreting numerical artifacts as streamer branches, the branching must be symmetric as well. Figure 5 shows one of these symmetric case studies in which the spatial distributions on the charge

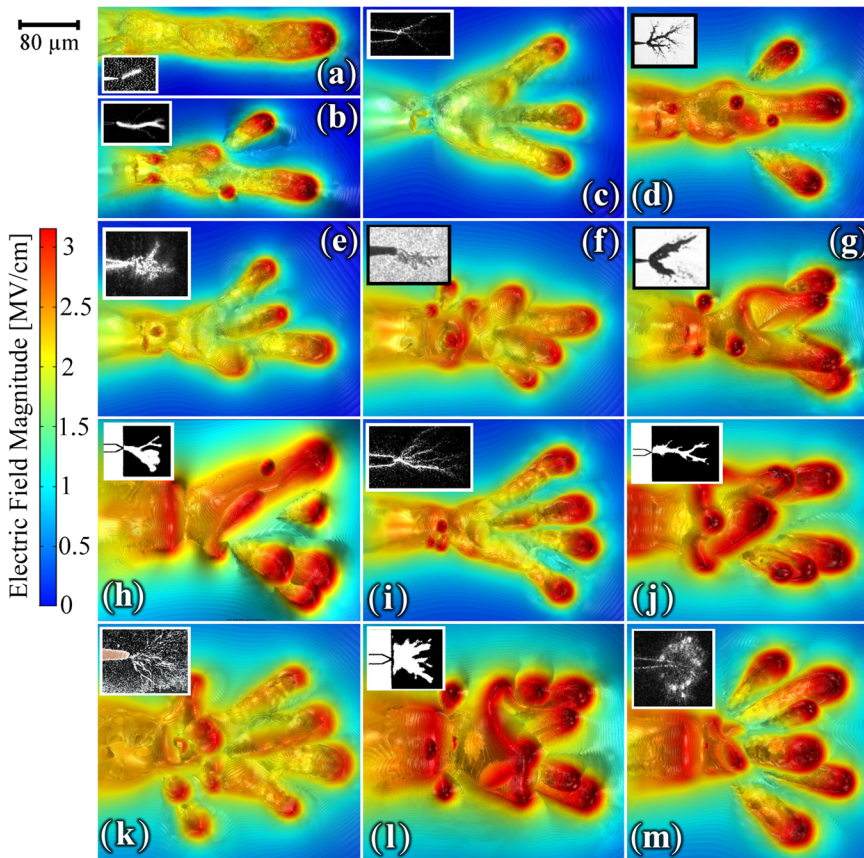


FIG. 4. Iso-surface plot of electric field distribution as modeling result of streamer is compared with corresponding experimental image in the inset image. Definite breakdown voltage, U_{DBD} , for the modeling geometry (gap length, $d = 25$ mm) is equal to 95 kV. The initiation voltage for the modeling geometry (electrode tip radius, $r_i = 40$ μ m) is 30 kV. In the experimental data, the applied voltages are expressed in terms of streamer initiation voltage, V_i , and 50% breakdown voltage, U_{BD} , which is the impulse peak at which the dielectric breaks down in half of the discharge tests. For each panel the modeling data is expressed, followed by brief information about the related experiment in Table II.

carrier densities are symmetrical to the plane, $y = 0$. The streamer branching results in the sanity checks successfully followed the symmetry of the inhomogeneities (e.g., as can be seen in Fig. 5 for a representative case), meaning that

numerical instabilities are not amplified by the system. Note that the three-dimensional mesh of the model is not symmetrical to the planes of symmetry (e.g., $y = 0$ in Fig. 5). If there were significant numerical noise amplifications in the

TABLE II. Key parameters of modeling and experimental cases shown in Figure 4. Initiation voltages, in all cases, are taken from Ref. 35.

| Modeling data (peak, rise time) | Experiment data obtained from literature (photography method and applied voltage) |
|---|--|
| (a) $2.85 V_i$ ($0.9 U_{DBD}$), 1 ns | Streak image of streamer formed by $2.18 V_i$ ($0.33 U_{50BD} = 327$ kV) in a 150 mm gap with $r_i = 1$ mm ($U_{50BD} \approx 970$ kV) ^{33,36} |
| (b) (a): $6 V_i$ ($1.9 U_{DBD}$), 100 ns | Streak image of streamer formed by $4.88 V_i$ ($1.57 U_{50BD} = 583$ kV) in a 100 mm gap with $r_i = 1$ mm ($U_{50BD} \approx 370$ kV) ^{33,36} |
| (c) (a): $7.66 V_i$ ($2.42 U_{DBD}$), 10 ns | Schlieren images of streamer formed by $7.25 V_i$ (100 kV = $5.55 U_{50BD}$, 30 ns) in a 2.5 mm gap with $r_i = 25$ μ m ($U_{50BD} \approx 18$ kV) ^{30,36} |
| (d) $8.66 V_i$ ($2.74 U_{DBD}$), 100 ns | Streak images of streamer formed by $8.2 V_i$ ($0.8 U_{50BD} = 24$ kV) in a 3 mm gap with $r_i = 5$ μ m ($U_{50BD} \approx 30$ kV) ^{18,36} |
| (e) $9 V_i$ ($2.84 U_{DBD}$), 10 ns | Schlieren images of streamer formed by $2.77 V_i$ (47 kV = $1.88 U_{50BD}$, 20 ns) in a 5 mm gap with $r_i = 25$ μ m ($U_{50BD} \approx 25$ kV) ^{30,36} |
| (f) $10.66 V_i$ ($3.37 U_{DBD}$), 100 ns | Shadowgraphy images of streamer formed by $11.1 V_i$ ($5.55 U_{50BD} = 100$ kV, 1.2 μ s) in a 2.5 mm gap with $r_i = 30$ μ m ($U_{50BD} \approx 14$ kV) ^{1,36} |
| (g) $11.33 V_i$ ($3.58 U_{DBD}$), 10 ns | Streak images of streamer formed by $10.23 V_i$ ($1.14 U_{50BD} = 30$ kV) in a 2 mm gap with $r_i = 5$ μ m ($U_{50BD} \approx 30$ kV) ^{18,36} |
| (h) $12.6 V_i$ ($4 U_{DBD}$), 10 ns | Intensifier gate photographs of streamer formed by $13.2 V_i$ ($0.9 U_{50BD} = 304$ kV) in a 200 mm gap with $r_i = 40$ μ m ($U_{50BD} \approx 340$ kV) ^{34,36} |
| (i) $10 V_i$ ($3.16 U_{DBD}$), 100 ns | Schlieren images of streamer formed by $7.25 V_i$ ($5.55 U_{50BD} = 100$ kV, 300 ns) in a 2.5 mm gap with $r_i = 25$ μ m ($U_{50BD} \approx 18$ kV) ^{30,36} |
| (j) 15.2 ($4.8 U_{DBD}$), 10 ns | Intensifier gate photographs of streamer formed by $16 V_i$ ($0.87 U_{50BD} = 304$ kV) in a 200 mm gap with $r_i = 3$ μ m ($U_{50BD} \approx 350$ kV) ^{34,36} |
| (k) $15.83 V_i$ ($5 U_{DBD}$), 100 ns | Shadowgraphy images of streamer formed by $14.44 V_i$ ($9.28 U_{50BD} = 130$ kV, 1.2 μ s) in a 2.5 mm gap with $r_i = 30$ μ m ($U_{50BD} \approx 14$ kV) ^{1,36} |
| (l) 16.1 ($5.1 U_{DBD}$), 10 ns | Intensifier gate photographs of streamer formed by $18.62 V_i$ ($1.38 U_{50BD} = 304$ kV) in a 50 mm gap with $r_i = 3$ μ m ($U_{50BD} \approx 220$ kV) ^{34,36} |
| (m) $18.3 V_i$ ($5.8 U_{DBD}$), 100 ns | Schlieren images of streamer formed by $20.1 V_i$ ($4.3 U_{50BD} = 28$ kV, 1 μ s) in a 1 mm gap with $r_i = 5$ μ m ($U_{50BD} \approx 6.5$ kV) ^{1,36} |

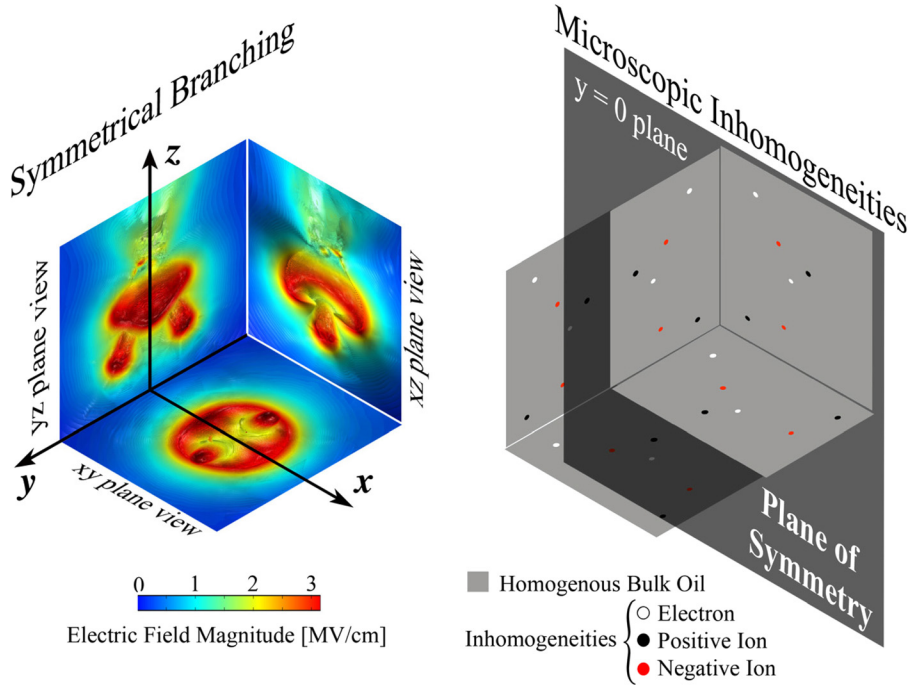


FIG. 5. Symmetrical streamer branching due to symmetric initial electron disturbance distribution (planes of symmetry are $x=0$ and $y=0$) showing that the numerical instabilities are minor enough to guarantee that the branching occurs due to physical inhomogeneities. The propagation direction of the main streamer column is in $-z$ direction. The left panel shows iso-surface plots of the electric field generated by streamer branching from different view planes (xy , xz , and xy plane views).

system, they would appear and disrupt the symmetry of the results.

B. Geometry of streamer head: Deterministic causes of branching

To better understand the underlying deterministic causes that make the streamer shell tear apart at the streamer head, we have studied the relationship between the branching dynamics and the structure of the streamer head to realize whether branching occurs and if it happens how many propagating branches come out of the main stem. To be able to quantify this relationship, we have defined three characteristic lengths: r_a , r_b and d based on the volume charge density distribution ($0.5\rho_{max}$ to ρ_{max}) and the head curvature ratio, $\alpha = r_a/d$, as shown in Fig. 6.

The streamer characteristic lengths are measured from the modeling results of 280 simulation case studies and classified based upon the number of propagating branches as shown in Fig. 7. Thin streamers usually have relatively thick shell of streamer head, which makes the propagating streamer unable to branch out even in inhomogeneous media for two main reasons:

1. Small r_a : The streamer head is $\sim 10\text{--}20\ \mu\text{m}$ thick which increases the probability that the streamer is not influenced by microscopic inhomogeneities unless the inhomogeneity density is extremely high. At the current inhomogeneity size, $5\ \mu\text{m}$, and density, $10^{11}\ \text{m}^{-3}$, the streamer takes some detour from its main path, rather than branching out, even if a spherical inhomogeneity is close to the streamer head, since the head is strongly stable.
2. Large d : The charge density at the streamer head is relatively high which considerably increases the streamer velocity. Since the higher the streamer velocity, the lower the branching probability, relatively large d along with small r_a assist the streamer not to branch out.

However, as the streamer column becomes thicker (r_a) and the streamer head crust (d) becomes thinner (as a result of higher applied voltage peak and/or rate of rise of voltage), there are some cases in which branching does not occur even though d and r_a are fairly small and large, respectively. Comparing the results plotted in Fig. 7 suggests that the important geometrical parameter that determines the number of just born branches is the head curvature ratio $\alpha = r_a/d$, not merely r_a , r_b , or d . This ratio seems to be controlled with the applied voltage characteristics and number density and

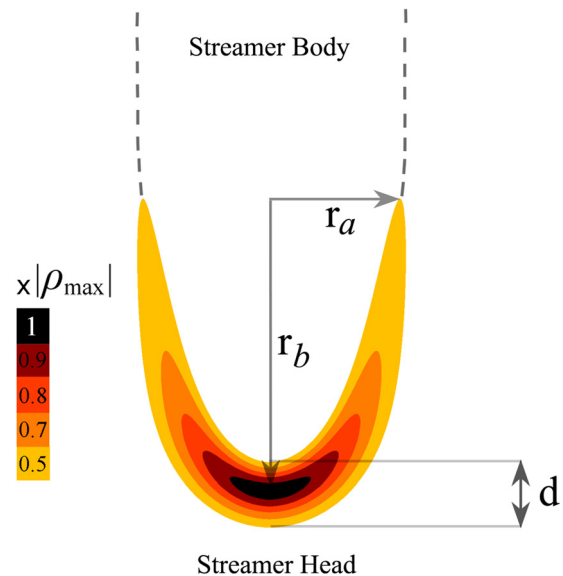


FIG. 6. Streamer head configuration. Three characteristic lengths, r_a , r_b , and d , are defined based on the volume charge density distribution ($0.5\rho_{max}$ to ρ_{max}) to study the streamer head instability growth, which ultimately causes the branching. Numerical modeling shows that the chance of branching increases as the head curvature ratio $\alpha = r_a/d$ increases. Our previous studies show that increasing either applied voltage peak or applied voltage rate of rise would increase α .

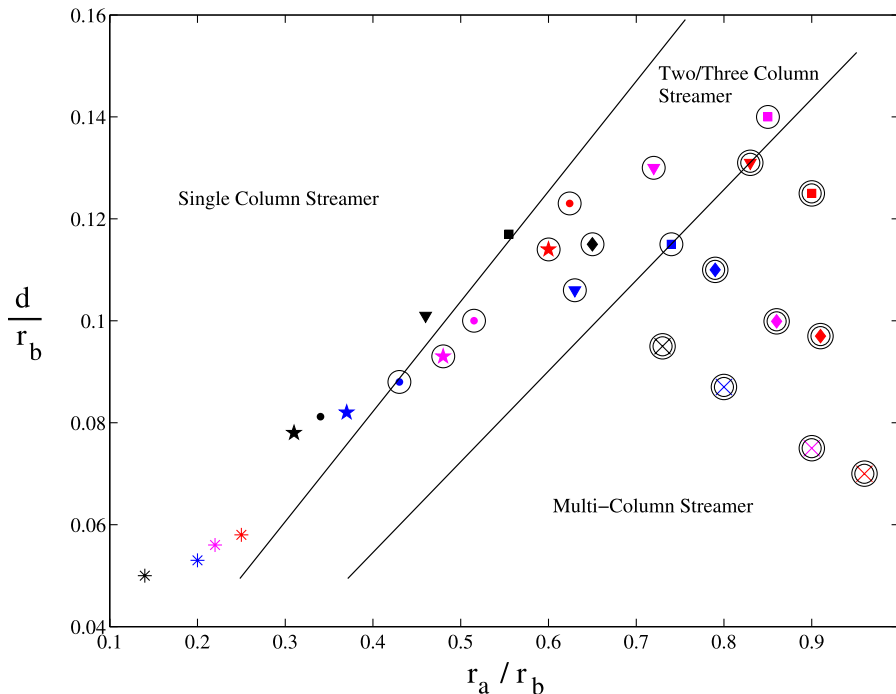


FIG. 7. Identification of streamer tree number of branches based on the streamer head geometry (characteristic lengths defined in Figure 6). Colors show the applied voltage rise-times: black (1 μ s), blue (100 ns), purple (10 ns), and red (1 ns). Marker shapes indicate the applied voltage peaks: 130 kV (*), 200 kV (\star), 250 kV (\bullet), 300 kV (\blacktriangledown), 350 kV (\blacksquare), 400 kV (\blacklozenge), and 500 kV (\times). The points are obtained from taking average from ten different inhomogeneity distributions, but with the same inhomogeneity radius, maximum intensity, and density of $5 \mu\text{m}$, 10^4Cm^{-3} , and 10^{11}m^{-3} , respectively.

intensity of the inhomogeneities. For a given inhomogeneity, before running the 3-D model, if we know the steady streamer head geometry, α approximately determines the number of the propagating branches. In Fig. 7, the separation lines between single column, two/three column and multi column streamers roughly show the critical head curvature ratio. The value of critical curvature ratio is controlled by density and intensity of the microscopic inhomogeneities. Particularly, if either density or intensity of the inhomogeneities increases, the critical streamer head curvature ratio will decrease (slope of the separation lines in Fig. 7 increase). Based on the results obtained from cases having different inhomogeneity densities and intensities, the critical head curvature is more sensitive to the perturbation density rather than the perturbation intensity.

There are a number of additional interesting discussions raised by observations made on the 3-D geometrical attributes of a streamer right at the branching:

- Streamer velocity drops just before branching begins. After branching, each individual branch accelerates again. In the two/three column streamer region (Fig. 7), one of the streamer branches usually picks up the maximum velocity which is clearly higher than other branch velocities. This maximum velocity agrees with experimental evidence found in the literature, even closer than the 2-D axisymmetric modeling results. However, for multiple column streamers (especially for four streamer branches or more), almost all of the child branches propagate with roughly similar velocity which is lower than the velocities reported in experimental records.^{1,2,4,28}
- For a given perturbation intensity, number and thickness of the streamer branches are determined by the applied voltage, unless its diameter is larger than a certain value. This threshold size in the presented perturbation density and intensity is $10 \mu\text{m}$. In other words, for inhomogeneity sizes

above $10 \mu\text{m}$, different applied voltages create almost similar streamer trees. This is particularly reasonable, since macroscopic inhomogeneities dominantly determine the streamer behavior. In terms of the visual resemblance between modeling results and experimental images as presented in Fig. 4, $5 \mu\text{m}$ inhomogeneities with density of 10^{11}m^{-3} on the charge carriers is optimal combination.

- Modeling results show that the spherical inhomogeneities (containing maximum charge perturbations of 10^4Cm^{-3}) that are farther than 1 mm from the path of the streamer do not effectively cause streamer deflections or branching. Therefore, as mentioned earlier, the inhomogeneities are limited to be distributed only inside the pillbox close to the streamer tip, and spherical inhomogeneities beyond those boundaries are ignored to avoid numerical difficulties (excessive simulation time).
- After the first branching, velocities of the branches increase which makes the secondary branching unlikely at least with the current magnitude of the perturbations. It has also been observed in experiments^{4,30} that the secondary branching does not happen unless the streamer branch travels over a certain distance from the original node. The ratio of branching length over streamer diameter of about 12 to 15, reported in Ref. 6, cannot be verified through the current version of the model due to computational limitations.
- Some of the case studies presented in this paper are repeated with inhomogeneities in oil permittivity with almost identical results. No significant difference was found in the branching triggered with the inhomogeneities on permittivity compared to those driven by inhomogeneities on charge density. We have examined water droplets, air bubbles (with higher, 80, and lower, 1, relative permittivities than oil, 2.2, respectively), and conductive dust particles as microscopic perturbations.¹³ The streamer crust is attracted to the bubbles with high conductivities or

higher permittivities (than oil), while low permittivity inhomogeneities repel the streamer head. A full discussion on the forces on the streamer head applied by the immersed objects in the liquid can be found in Ref. 22.

- The streamer diameters in the experimental images can be estimated to be about half of the electrodynamic diameter.⁶ Therefore, the modeling results describe the streamer branch's column diameters precisely. In general, streamer photography using different approaches such as Charge Coupled Device photography, Schlieren and Shadowgraphy,^{25,33,34} is extremely difficult to use for study of streamer branching due to small dimensions and high velocities of streamers. An interesting stereophotographic approach to resolve streamer in air is presented in Ref. 12. In most of these studies, the scientific goal is to capture streamer trees with the most possible branches. Therefore, the applied voltage and camera shooting times have been set to guarantee a high number of branches, which makes it difficult to find the branching threshold through the images. In addition, what the streak cameras capture are not the ionized body of the streamer, but the path of the emitted light, which is most probably path of dissipated energy (via joule heating for instance). Experimental photography is more useful to understand the fractal structure of the streamer tree not the branching phenomena itself.¹⁴ Therefore, it seems the 3-D modeling is currently the best practical way to study the branching phenomena.
- This paper focuses on the streamer branching in liquids. In other media, other processes may become critically important in streamer acceleration and branching. For instance in gaseous environment, other than stochastic charge density fluctuations, in intense electric field, run-away electrons can contribute to accelerating and branching of streamers.⁷ A 3-D gaseous hybrid model is developed in Ref. 10 that couples a particle model for single electrons in the region of high fields and low electron densities with a fluid model in the rest of the domain.
- According to the current thermal simulations and experimental evidence, more realistic models of streamers in transformer oil must include a gas phase (vapor) and low temperature collisional plasma phase over a temperature range from 300 to 2000 K.³⁶ However, previous experience³⁷ in simulating phase conversion (including a plasma phase) in COMSOL Multiphysics²³ indicates that it is extremely difficult to combine the entire plasma equation set with the pre-breakdown equations (Eqs. (1)–(7)) with an acceptable convergence, especially in a 3-D geometry.
- In addition to inhomogeneities in the dielectric volume, the small cracks, and perturbations on the needle electrode should be addressed in the future. Some of experimental images show that branching has started right at the needle itself.³⁰

V. CONCLUDING REMARKS

A fully three-dimensional model of streamers is employed to investigate the dynamics of streamer branching, which is an asymmetric phenomenon by its nature. The

modeling results show that the streamer branching has deterministic origins, as well as stochastic roots. Specifically, if the volume charge layer at the streamer head is thin and slow enough, even an infinitesimal inhomogeneity is sufficient to trigger the branching. On the other hand, if the streamer head is stable, even relatively large perturbations do not grow instabilities from the streamer head. We have derived a quantitative gauge for the streamer head geometry that determines whether branching occurs under specific inhomogeneous circumstances. The critical ratio of the streamer charge sheath thickness over the streamer width, at which branching occurs, is found for the specific density and intensity of inhomogeneities. Comparing the modeling results with corresponding experimental images indicates that the model predicts the branching phenomena both quantitatively and qualitatively. In terms of the visual resemblance between modeling results and experimental images, 5 μm spherical inhomogeneities with spatial number density of 10^{11} m^{-3} is an optimal combination in transformer oil.

ACKNOWLEDGMENTS

This work was supported by ABB Corporate Research, Västerås, Sweden, the IEEE Nuclear and Plasma Sciences Society, and the IEEE Dielectrics and Electrical Insulation Society.

¹A. Beroual, M. Zahn *et al.*, "Propagation and structure of streamers in liquid dielectrics," *IEEE Electr. Insul. Mag. (USA)* **14**, 6–17 (1998).

²G. Massala and O. Lesaint, "Positive streamer propagation in large oil gaps: Electrical properties of streamers," *IEEE Trans. Dielectr. Electr. Insul.* **5**(3), 371–381 (1998).

³J. Jadidian, M. Zahn, N. Lavesson, O. Widlund, and K. Borg, "Effects of impulse voltage polarity, peak amplitude and rise-time on streamers initiated from a needle electrode in transformer oil," *IEEE Trans. Plasma Sci.* **40**(2), 909–918 (2012).

⁴O. Lesaint and M. Jung, "On the relationship between streamer branching and propagation in liquids: Influence of pyrene in cyclohexane," *J. Phys. D: Appl. Phys.* **33**, 1360–1368 (2000).

⁵L. Papageorgiou, A. C. Metaxas, and G. E. Georghiou, "Three-dimensional numerical modelling of gas discharges at atmospheric pressure incorporating photoionization phenomena," *J. Phys. D: Appl. Phys.* **44**, 045203 (2011).

⁶A. Luque and U. Ebert, "Electron density fluctuations accelerate the branching of positive streamer discharges in air," *Phys. Rev. E* **84**, 046411 (2011).

⁷K. Niayesh, E. Hashemi, E. Agheb, and J. Jadidian, "Sub-nanosecond breakdown mechanism of low pressure gaseous spark gaps," *IEEE Trans. Plasma Sci.* **36**, 930–931 (2008).

⁸J. Townsend, *The Theory of Ionization of Gases by Collision* (Constable & Company, London, 1910).

⁹N. Davari, P.-O. Åstrand, and T. Van Voorhis, "Field-dependent ionization potential by constrained density functional theory," *Mol. Phys.* (to be published).

¹⁰C. Li, J. Teunissen, M. Nool, W. Hundsdoerfer, and U. Ebert, "A comparison of 3D fluid, particle and hybrid model for negative streamers," *Plasma Sources Sci. Technol.* **21**, 055019 (2012).

¹¹T. M. P. Briels *et al.*, "Positive and negative streamers in ambient air: measuring diameter, velocity and dissipated energy," *J. Phys. D: Appl. Phys.* **41**, 234004 (2008).

¹²S. Nijdam, "Experimental investigations on the physics of streamers," Ph.D. dissertation (Technische Universiteit Eindhoven, 2011).

¹³N. Y. Babaeva and M. J. Kushner, "Streamer branching: The role of inhomogeneities and bubbles," *IEEE Trans. Plasma Sci.* **36**(4), 892–893 (2008).

¹⁴H. A. Fowler, J. E. Devaney, and J. G. Hagedorn, "Growth model for filamentary streamers in an ambient field," *IEEE Trans. Dielectr. Electr. Insul.* **10**(1), 73–79 (2003).

- ¹⁵J. Qian, R. P. Joshi, E. Schamiloğlu, J. Gaudet, J. R. Woodworth, and J. Lehr, "Analysis of polarity effects in the electrical breakdown of liquids," *J. Phys. D: Appl. Phys.* **39**, 359–369 (2006).
- ¹⁶M. Zahn, "Dynamics of stratified liquids in the presence of space charge," *Phys. Fluids* **15**, 1408–1417 (1972).
- ¹⁷M. Zahn, "Space charge coupled interfacial waves," *Phys. Fluids* **17**, 343–352 (1974).
- ¹⁸W. G. Chadband, "On variations in the propagation of positive discharges between transformer oil and silicone fluids," *J. Phys. D: Appl. Phys.* **13**, 1299–1307 (1980).
- ¹⁹F. O'Sullivan, "A model for the initiation and propagation of electrical streamers in transformer oil and transformer oil based nanofluids," Ph.D. dissertation (Massachusetts Institute of Technology, 2007).
- ²⁰J. G. Hwang, "Elucidating the mechanisms behind pre-breakdown phenomena in transformer oil systems," Ph.D. dissertation (Massachusetts Institute of Technology, 2010).
- ²¹J. Jadidian, M. Zahn, N. Lavesson, O. Widlund, and K. Borg, "Impulse breakdown delay in liquid dielectrics," *Appl. Phys. Lett.* **100**, 192910 (2012).
- ²²J. Jadidian, M. Zahn, N. Lavesson, O. Widlund, and K. Borg, "Surface flashover breakdown mechanisms on liquid immersed dielectrics," *Appl. Phys. Lett.* **100**, 172903 (2012).
- ²³Reference guide, COMSOL Multiphysics 4.3a.
- ²⁴W. F. Schmidt, *Liquid State Electronics of Insulating Liquids* (CRC Press, 1997).
- ²⁵D. S. Sholl and J. A. Steckel, *Density Functional Theory, a Practical Introduction* (John Wiley & Sons, Inc., New Jersey, 2009).
- ²⁶C. Zener, "A theory of the electrical breakdown of solid dielectrics," *Proc. R. Soc. A* **145**, 523–529 (1934).
- ²⁷IEC Standard #60060-1, "High-voltage test techniques - Part 1: General definitions and test requirements."
- ²⁸M. Zahn, *Electromagnetic Field Theory: A Problem Solving Approach* (Robert E. Krieger, Inc., 2003).
- ²⁹R. Codina, "A discontinuity-capturing cross-wind-dissipation for the finite element solution of the convection-diffusion equation," *Comp. Methods Appl. Mech. Eng.* **110**, 325–342 (1993).
- ³⁰M. D. Cevallos, "Phenomenological investigation of breakdown in oil dielectrics," Ph.D. dissertation (Texas Tech University, Lubbock, TX, 2005).
- ³¹IEC Standard #60897, "Methods for the determination of the lightning impulse breakdown voltage of insulating liquids."
- ³²R. Liu, *Needle-Sphere Transformer Oil Breakdown Experimental Setup* (ABB Corporate Research, Västerås, Sweden, 2010).
- ³³L. Lundgaard, D. Linhjell, G. Berg, and S. Sigmond, "Propagation of positive and negative streamers in oil with and without pressboard interfaces," *IEEE Trans. Dielectr. Electr. Insul.* **5**(3), 388–395 (1998).
- ³⁴P. Rain and O. Lesaint, "Prebreakdown phenomena in mineral oil under step and ac voltage in large-gap divergent fields," *IEEE Trans. Dielectr. Electr. Insul.* **1**(4), 692–701 (1994).
- ³⁵O. Lesaint and T. V. Top, "Streamer initiation in mineral oil, Part I: Electrode surface effect under impulse voltage," *IEEE Trans. Dielectr. Electr. Insul.* **9**, 84–91 (2002).
- ³⁶J. Jadidian, "Charge transport and breakdown physics in liquid/solid insulation systems," Ph.D. dissertation (Massachusetts Institute of Technology, 2013).
- ³⁷J. Jadidian, S. Mohseni, M. Jebeli-Javan, E. Hashemi, A. A. Shayegani, and K. Niayesh, "Visualization of a copper wire explosion in atmospheric pressure air," *IEEE Trans Plasma Sci.* **39**, 2842–2843 (2011).